Optimality and adaptation of phenotypically switching cells in fluctuating environments

Merzu Kebede Belete and Gábor Balázsi

Optimality and Adaptation of Phenotypically Switching Cells in Fluctuating Environments

Merzu Kebede Belete[1,2,3] & Gábor Bálazsi[1,2*]

[1] *Laufer Center for Physical and Quantitative Biology, Stony Brook University, Stony Brook, New York, United States of America.*
[2] *Department of Biomedical Engineering, Stony Brook University, Stony Brook, New York, United States of America.*
[3] *Department of Physics, University of Houston. Houston, Texas, United States of America.*

Stochastic switching between alternative phenotypic states is a common cellular survival strategy during unforeseen environmental fluctuations. Cells in different subpopulations proliferate at different rates in different environments. Optimal population growth is typically assumed to occur when phenotypic switching rates match environmental switching rates. However, it is not well understood how this optimum behaves as a function of the growth rates of phenotypically different cells. In this study, we use mathematical and computational models to test how the actual parameters associated with optimal population growth differ from those assumed to be optimal. We find that the predicted optimum is practically always valid if the environmental durations are long. However, the regime of validity narrows as environmental durations shorten, especially if subpopulation growth rate differences differ from each other (are asymmetric) in two environments. Furthermore, we study the fate of mutants with switching rates previously predicted to be optimal. We find that mutants which match their phenotypic switching rates with the environmental ones can only sweep the population if the assumed optimum is valid, but not otherwise.

I. Introduction

Cell populations experience countless environmental changes, from simple periodic day-night cycles to unpredictable exposures to nutrients, antibiotics, pH or temperature shifts. One possible way to survive in such unpredictable environmental fluctuations is to generate phenotypic heterogeneity in the cell population [1–7]. Generation of heterogeneity is a broadly observed bet-hedging strategy of various systems operating in unpredictable environments, ranging from financial markets [8] to bacteria and viruses, including the lysis-lysogeny switch of phage lambda [9, 10], lactose utilization [11] and chemotaxis in *Escherichia coli* [12], phase variation in a number of pathogens [13, 14], cellular differentiation in *Bacillus subtilis* [15, 16], bacterial persistence [1], among many other examples.

Cells in phenotypically heterogeneous populations can switch from one phenotype to another [6, 17]. Previous theoretical studies have shown that a phenotypically heterogeneous population can achieve maximal growth rate if its phenotype switching rates match the environmental switching rates. These earlier studies assumed that environmental durations are long compared to phenotypic switching times, and that each environment favors a particular phenotype [18, 19], such that cells with the given phenotype grow fastest in that environment. Although widely accepted, it is unclear whether cellular and environmental switching rates must always match for the population growth rate to be optimal. Indeed, recent theoretical work introduced corrections to the assumed optimum [20]. In particular, how the existence of the assumed optimum depends on each phenotype's growth rates in each environmental condition has not been investigated. Likewise, it is unclear how the validity of the assumed optimum depends on the rates of environmental fluctuations.

In this paper, we mathematically explore the parameter space of each phenotype's growth rates to determine how the assumed optimum differs from the actual optimum. We find many parameter combinations where the computed optimum differs from the assumed optimum. As expected considering the assumptions of the earlier models, the actual and assumed optima are practically identical for a wide parameter range if the environmental durations are long compared to the growth rates, but not otherwise. Specifically, we find that the validity of the computed optimum depends on the growth rates of individual phenotypes in each environment. Finally, we study the fate of mutants with phenotypic switching rates assumed to be optimal (i.e., matching the environmental switching rates) in populations with nonoptimal phenotype switching rates. We find that such mutants can sweep the population only if the assumed optimum is valid. In other cases, when the assumed optimum is invalid, the mutant does not sweep the population even though its phenotypic switching rates match the environmental switching rates.

The paper is structured as follows. First, we present a deterministic and stochastic mathematical model to address the question of growth optimality in fluctuating environments. Second, we derive a general analytic solution for the population growth rate. We then use these models to study the optimum in the parameter space of each phenotype's growth rates in each environment. Next, we introduce a mutant with switching rates matching those of the environment in populations with different phenotype switching rates, and study its evolutionary dynamics. Finally, we present our conclusions.

II. Models of phenotypically heterogeneous populations

For simplicity, we consider a clonal population where individual cells can switch between two distinct phenotypic states (*type I* and *type II*) as shown in Figure 1(A & B). Likewise, we consider that the environment can be in two different states that alternate periodically in time (Figure 1(C)). This simplification can be generalized to any number of phenotypes and environmental states as it was done

* gabor.balazsi@stonybrook.edu

previously [19].

A. Deterministic mathematical model

In the mathematical model, we allow cells to switch randomly from type j to type i with switching rate ω_{ij} independent of the environments, ε_m. Moreover, the environment switches from state m to state n with switching rates ε_{nm}. The growth rates, $g_i(\varepsilon_m)$, depend on the environment as shown in Figure 1. The equation dictating the dynamics of the population is given by the time derivative of the population state vector, $\mathbf{X}(t)$, in Equation (1).

$$\frac{dX_i}{dt} = s_{ij}(\varepsilon)X_j, \tag{1}$$

where $s_{ij}(\varepsilon)$ are elements of the matrix,

$$\mathbf{S}(\varepsilon) = \begin{bmatrix} g_1(\varepsilon) - \omega_{21} & \omega_{12} \\ \omega_{21} & g_2(\varepsilon) - \omega_{12} \end{bmatrix}.$$

Since the growth rates depend on environments, the diagonal elements s_{ij} also depend on the environment. The above linear system of ordinary differential equations has a simple solution of the form

$$\mathbf{X}(\varepsilon,t) = c_1\mathbf{V}_1(\varepsilon)\exp(\lambda_1(\varepsilon)t) + c_2\mathbf{V}_2(\varepsilon)\exp(\lambda_2(\varepsilon)t), \tag{2}$$

where c_1 and c_2 are constants determined by the initial conditions (see Appendix), while $\lambda_1(\varepsilon)$ and $\lambda_2(\varepsilon)$ are the eigenvalues corresponding to the eigenvectors $\mathbf{V}_1(\varepsilon)$ and $\mathbf{V}_2(\varepsilon)$ of $\mathbf{S}(\varepsilon)$, respectively.

We solve Equation (1) for periodically alternating environments for either normal cells or 1 mutant cell among $N_0 - 1$ normal cells. We initiate the simulations with $N_0 = 10^4$ cells distributed equally between the two phenotypes. We maintain the population size constant throughout the simulations. The cells grow in environment i for a duration of τ_i and then the environment switches its state, imposing different growth rates for each phenotype for a duration of τ_j. We consider the phenotypic switching rates of mutants to be equal to the environmental switching rates, $(\omega_{ij} = \frac{1}{\tau_j})$. That is, the mutant cell matches its switching rates to the environmental switching rates. We then calculate the population fitness, $G(t)$, as a weighted average of cellular fitness values, $g_i(\varepsilon)$, by determining the fraction of cells, $f_i(\varepsilon)$, in each subpopulation in the given environment as

shown in Equation (3).

$$G(\varepsilon,t) = \sum_{i=1}^{2} f_i(\varepsilon,t)g_i(\varepsilon). \tag{3}$$

We averaged $G(\varepsilon,t)$ over one period, $(\tau_1 + \tau_2)$, once it stabilized (changed identically through two environmental periods) as shown in Figure 1(D).

B. Stochastic simulations

Stochastic simulations were based on Equation (1), which we considered as a stochastic processes, and simulated using a Constant-Number Monte Carlo approach [21–24]. Initially, we assigned $N_0 = 10^4$ cells equally distributed in the two states from a two-valued distribution. We maintained the population size constant throughout the simulations. Then, we allowed cells to randomly divide with growth rates $g_i(\varepsilon_m)$, and to switch with rates ω_{ij} corresponding to the given environment for a duration of τ_m. Then we repeated these steps after the environment switched to its other state for a duration of τ_n in ε_n. We continued the simulation by changing environments until the overall population growth looked practically identical within two successive environmental periods $(\tau_m + \tau_n)$. The population fitness is defined by the exponential growth rate, calculated as the average increment in the number of cells in a given generation time divided by the total number of cells entering the generation time.

C. Identifying the fitness optimum

We mapped the population fitness landscape as function of the phenotypic switching rates for both models (stochastic and deterministic). We searched the fitness landscape for the optimum fitness while varying the environmental durations. If the assumed optimum value exists, it must be inside the landscape either matching the environmental switching rates or shifted from the predicted value (hypothesis). We defined this relative shift in position as $R = \frac{\sqrt{(\omega^s_{12} - \omega^p_{12})^2 + (\omega^s_{21} - \omega^p_{21})^2}}{\sqrt{(\omega^p_{12})^2 + (\omega^p_{21})^2}}$, where ω^s_{ij} and $\omega^p_{ij} = \frac{1}{\tau_j}$ are the optimal switching rates for the simulation and theoretical assumption [19], respectively. If the optimum fell on the edge of the landscape (where at least one phenotypic switching rate is zero), we considered the assumed optimum to be invalid. We scanned the growth rates for each phenotype in each environment by setting $g_1(\varepsilon_1)$ to be the maximum fitness for the first environment, and keeping it constant. Then we looked for the fitness optimum while varying each other growth rate as described above.
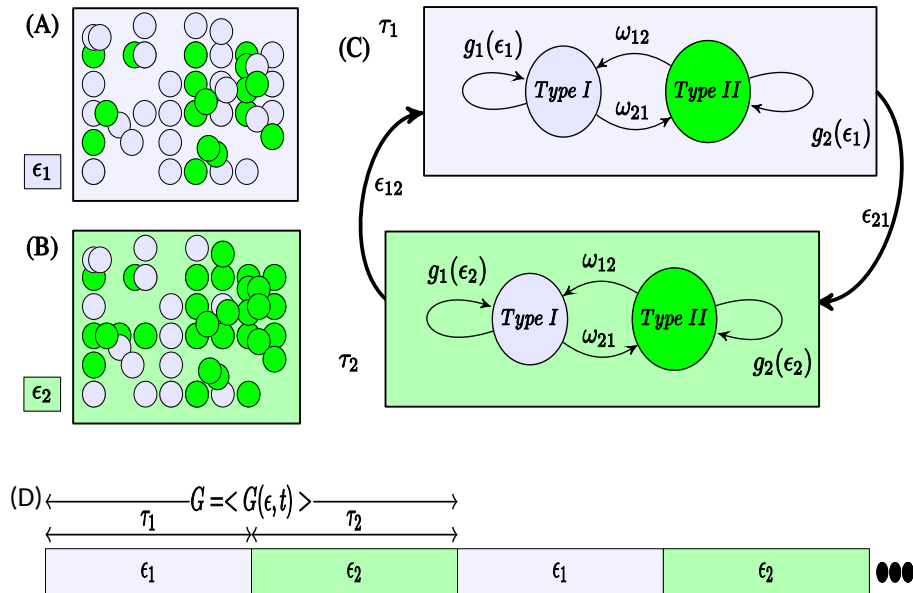
Figure 1. (Color), A two-state Markov chain model of phenotypic switching in an environment fluctuating between two different states, ε_1 and ε_2. Cells switch phenotypes between *Type I* and *Type II*. (A) Environment ε_1 favors the grey *Type I* cells, and (B) environment ε_2 favours the green *Type II* cells. (C) The cells grow with growth rates $g_i(\varepsilon_1)$ and switch from phenotype j to phenotype i with rate ω_{ij} in environment ε_1 that lasts for a time τ_1. Then the cells grow with growth rate $g_i(\varepsilon_2)$ in environment ε_2 that has a time duration τ_2. (D) Averaging the time dynamics of the population fitness in fluctuating environments. The cells grow in environment 1 for duration τ_1 and then the environment switches to environment 2, imposing different growth rates for each phenotype for a duration τ_2. The switching of environments were carried out for sufficiently long time so that the distribution of the number of cells in each state is identical for two consecutive periods. One period lasts for $\tau_1 + \tau_2$ duration of time. The time varying population fitness, $G(\varepsilon, t)$, is averaged over one such period after the distribution is stabilized.

III. Results
A. Testing the validity of the assumed optimum

It has been shown previously and it is widely accepted that the growth rate of phentypically switching cell populations is optimal when the phenotypic switching rates match the environmental switching rates. However, the conditions for the existence of this optimum are not well understood. Specifically, it is unclear if the assumed optimum occurs independently of each phenotype's proliferation rate in different environments. We tested this for various sets of growth rates. For symmetric growth rate combinations, where each environment enhances the fitness of a corresponding phenotype and suppresses the other equally (Figure 2 panel (A)), both the stochastic (upper row) and deterministic (lower row) models produced population fitness optima that was only slightly shifted from the assumed optimum. This small shift might arise from ignoring the higher-order terms in the theoretical prediction for short envi-

ronmental durations [20]. However, for a more asymmetric choice of growth rates (where one of the environments suppresses the fitnesses of both phenotypes) the position of the population growth optimum shifted substantially away from its assumed optimum, at matching phenotypic and environmental switching rates (Figure 2 panel (B)). For even more asymmetric growth rate combinations, the actual optimum moved to the edge of the fitness landscape (Figure 2 panel (C)) with $\omega_{12} = 0$. We will refer to this situation (when the optimum is on the edge of the fitness landscape) as "invalid assumption". On the other hand, we will refer to the situation when the optimum shifts, but still occurs inside the fitness landscape as "inaccurate assumption".

We keep fixed the growth rate of phenotype I in environment 1 at $(g_1(\varepsilon_1) = 0.50)$ and vary the other growth rates ($g_2(\varepsilon_1)$, $g_1(\varepsilon_2)$, and $g_2(\varepsilon_2)$).
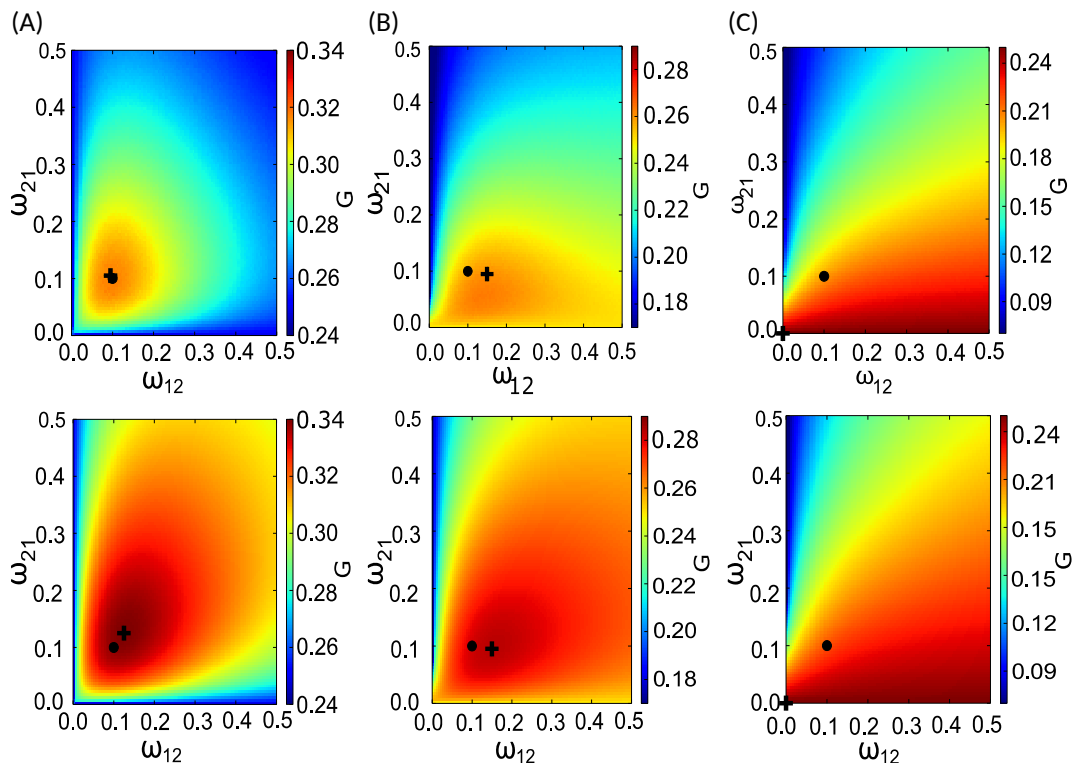
Figure 2. (Color), Optimal switching rates do not always match the environmental switching rates for $\tau_1 = \tau_2 = 10$ ($\bullet$ and $+$ indicate optimum points for the assumed and actual fitness optima, respectively). Panel (A) corresponds to symmetric growth rates $[(g_1(\varepsilon_1), g_2(\varepsilon_1)) = (0.50, 0.0001), (g_1(\varepsilon_2), g_2(\varepsilon_2)) = (0.0001, 0.50)]$. Panel (B) corresponds to asymmetric growth rates with parameter values $[(g_1(\varepsilon_1), g_2(\varepsilon_1)) = (0.50, 0.0001), (g_1(\varepsilon_2), g_2(\varepsilon_2)) = (0.0001, 0.3250)]$, where the actual optimum shifts away from the assumed one, as indicated by both stochastic (upper row) and deterministic (lower row) models. We refer to this situation as "inaccurate assumption". Finally, Panel (C) shows "invalid assumption" $[(g_1(\varepsilon_1), g_2(\varepsilon_1)) = (0.50, 0.0001), (g_1(\varepsilon_2), g_2(\varepsilon_2)) = (0.0001, 0.1251)]$, where the actual optimum is on the edge of the fitness landscape. The color bar indicates the population growth rate (fitness). We observed that if $N_0 < 100$, the optimum is not precisely localized due to genetic drift.

The difference between the stochastic and the deterministic models in Figure 2, especially at small growth rates, such as $[(g_1(\varepsilon_1), g_2(\varepsilon_1)) = (0.50, 0.0001), (g_1(\varepsilon_2), g_2(\varepsilon_2)) = (0.0001, 0.50)]$, compared to the switching rates arises because in the stochastic model, the population size is kept constant ($N_0 = 10^4$), which is implemented adding at most 1 cell at each time step in the simulation. By contrast, in the deterministic model we can have infinitely large population sizes accurately capturing slow growth in the population.

B. Exploring the parameter space: testing the validity of the assumed fitness optimum

As we have shown in Figure 2, a population can be closer or farther from the assumed fitness optimum by reversibly switching between phenotypic states. However, it is unclear how the lengths of environmental durations (long or short compared to the inverse of growth rates) affect this shift away from the assumption. Moreover, it is unknown how the growth rates of each phenotype affect the shift of the actual optimum relative to the assumed one. To address these questions, we studied the location of the maximum population fitness in the (ω_{12}, ω_{21}) space while scanning the growth rates of each phenotype in each environment (except for $g_1(\varepsilon_1)$, which we kept fixed). We studied systematically whether the actual fitness maximum was on the edge (invalid assumption) or substantially shifted (inaccurate assumption). To illustrate this, we plotted the shift as the relative distance, R of the actual optimum from the

assumed optimum versus the growth rates, $g_1(\varepsilon_2)$ and $g_2(\varepsilon_2)$ for several choices of $g_2(\varepsilon_1)$ and environmental durations. For long environmental durations there was a wide parameter regime where the optimum fitness occurred (Figure 3(C)) almost as assumed [19]. As the environmental durations decreased (Figure 3A & B), the shift became more pronounced, and the parameter regime where the assumed optimum fitness was valid narrowed. Moreover, the validity of the assumed optimum also depended on the choices of growth rates for each phenotype.

We observed that if the relative cellular growth rate differences ($\Delta_1 = g_1(\varepsilon_1)$ - $g_2(\varepsilon_1)$ & $\Delta_2 = g_2(\varepsilon_2)$ - $g_1(\varepsilon_2)$) differ substantially from each other (are asymmetric), the actual optimum moves away from the assumed optimum and eventually reaches the edge of the landscape (invalid assumption). This is especially true if growth rates are highly asymmetric in the two environments (for example, if one of the environments lowers both growth rates, while the other lowers only one). As shown in Figure 3(D), if the relative cellular growth rate differences are comparable, the existence of non-zero optimal switching rates depends crucially on both the symmetry of the growth rates and the length of the environmental durations. Specifically, if relative cellular growth rate differences do not differ much and the environmental durations are long, the optimal phenotypic switching rates match the environmental switching rates. However, for similar relative cellular growth rate differences, the

optimal regime shrinks and eventually it extends only along the diagonal where growth rates are symmetric. Even for the special case

of symmetric environments ($\Delta_1 = \Delta_2$), the actual optimum position shifts farther from the assumed one as the relative growth rate differences become smaller. These results are shown in Figure 3(D).
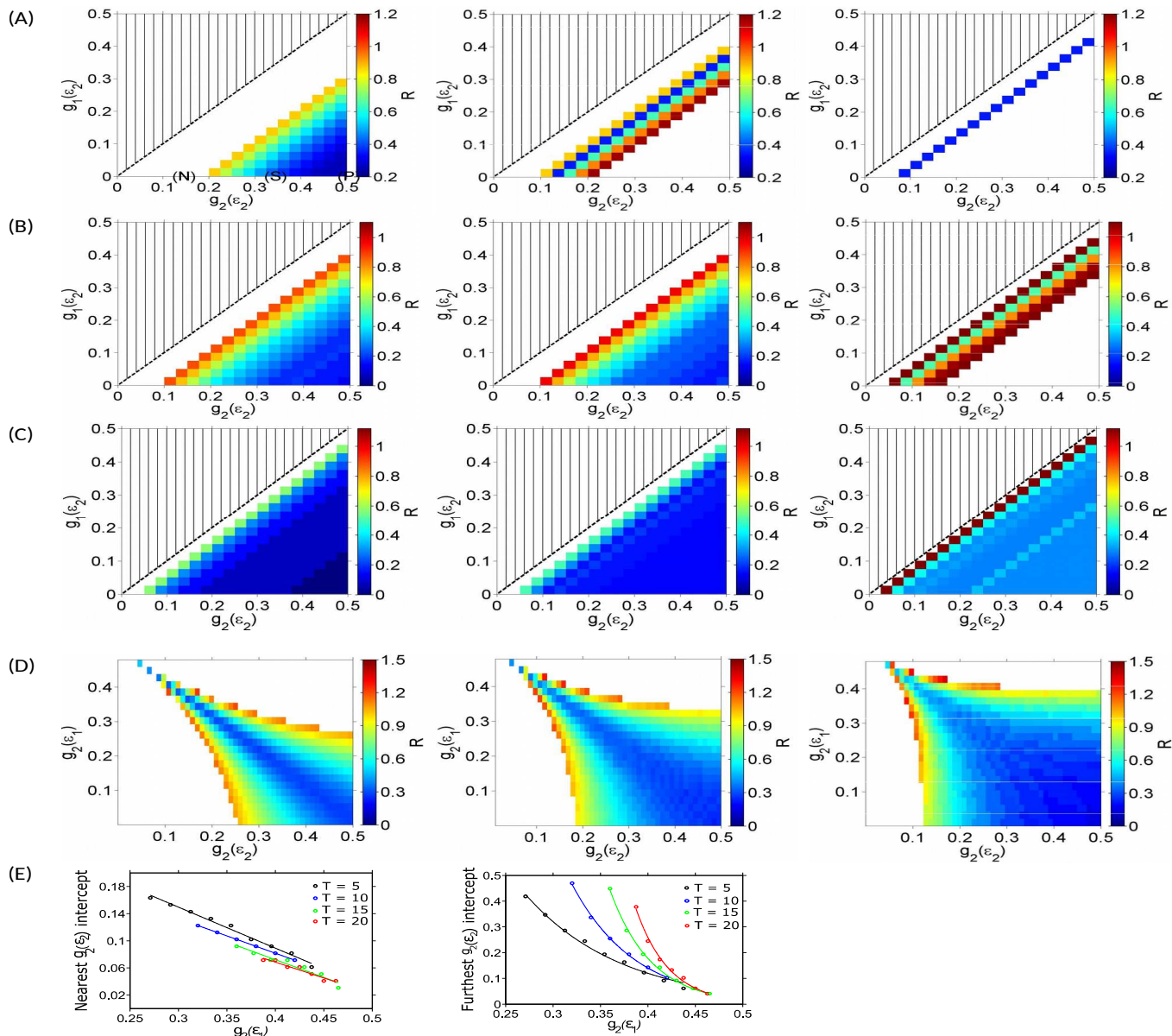

Figure 3. (Color), Validity and accuracy of assumed optimum in the parameter space. The smooth white region indicates that the assumption is invalid. The hashed region indicates that the optimum occurs for switching rates equal to zero. The rows of panels (A, B, C) correspond to different environmental durations with growth rates $g_1(\varepsilon_1) = 0.50$ and $g_2(\varepsilon_1) = [0.0001\ 0.375\ 0.425]$, respectively. (A) Validity of the assumed optimum for environmental duration $\tau_1 = \tau_2 = 10$. The point marked "P" corresponds to panels (A) in Figure 2 and Figure 4(A) where the assumed optimum occurs practically as predicted. The point marked by "S" corresponds to panels (B) in Figure 2 and (B) in Figure 4 where the optimum is shifted. Finally, point "N" corresponds to panels (C) in Figure 2 and (C) in Figure 4 where the assumed optimum is invalid. (B) Validity of the assumed optimum for environmental durations $\tau_1 = \tau_2 = 25$. (C) Validity of the assumed optimum for environmental durations $\tau_1 = \tau_2 = 100$. We keep fixed the growth rate of phenotype I in environment 1 at ($g_1(\varepsilon_1) = 0.50$) and vary the other growth rates ($g_2(\varepsilon_1)$, $g_1(\varepsilon_2)$, and $g_2(\varepsilon_2)$). The color indicates the relative shift in the position of the optimum relative to the assumed position. (D) The phase space where the optimum exists for $[g_1(\varepsilon_1) = 0.5, g_1(\varepsilon_2) = 0.0001]$ for environmental durations of $\tau_1 = \tau_2 = 5$, 10 & 20, respectively. (E) The $g_2(\varepsilon_2)$ intercepts where the optimum becomes invalid in panel D. The intercepts correspond to the point where the optimality assumption becomes invalid. The first intercept decreases approximately linearly whereas the second intercepts decays exponentially with the parameter values given in table I. The solid lines are least-squares fits and the dots are the actual points extracted from the phase space in panel D.

C. Evolutionary dynamics of phenotypic Sswitching rate mutants

Phenotypic switching rates could be subject to change due to mutations. Phenotypic switching rate mutants whose fitness is higher than that of the ancestral cell type should take over the population.

Here we consider a mutant that matches its phenotypic switching rates to environmental fluctuations. This mutant arises among cells that do not match their phenotypic switching rates to the fluctuating environment. In Figure 4 we plot the fraction of mutant cells having growth rates corresponding to points (N, S, P) on Figure 3 and switching rate $\frac{1}{\tau}$. Then in subsequent figures we plot the fraction of such phenotypic switching rate mutants in ancestral populations with various phenotypic switching rates over time. We find that the fraction of phenotypic switching rate mutants increases over time, indicating that the mutant can sweep almost all ancestral populations (Figure 4 (panel A)) when the assumed optimum is nearly valid (Figure 3(A), point P). However, when the predicted optimum is inaccurate or invalid (Figure 3(A), point S & N), mutants with the same switching rates do not sweep the ancestral population, as shown in Figure 4(B & C).

In small, reproductively isolated populations, rapid changes can occur in population structure. These changes are totally independent of natural selection. These changes are due solely to random cell division imposed on a constant-number population size over many generations. The smaller the population size, the more susceptible it becomes to random changes [25] 4(E). We found that a mutant, which matches its switching rates with the environmental switching rates still has higher chance of taking over the population despite random genetic drift, as shown in Figure 4(D).
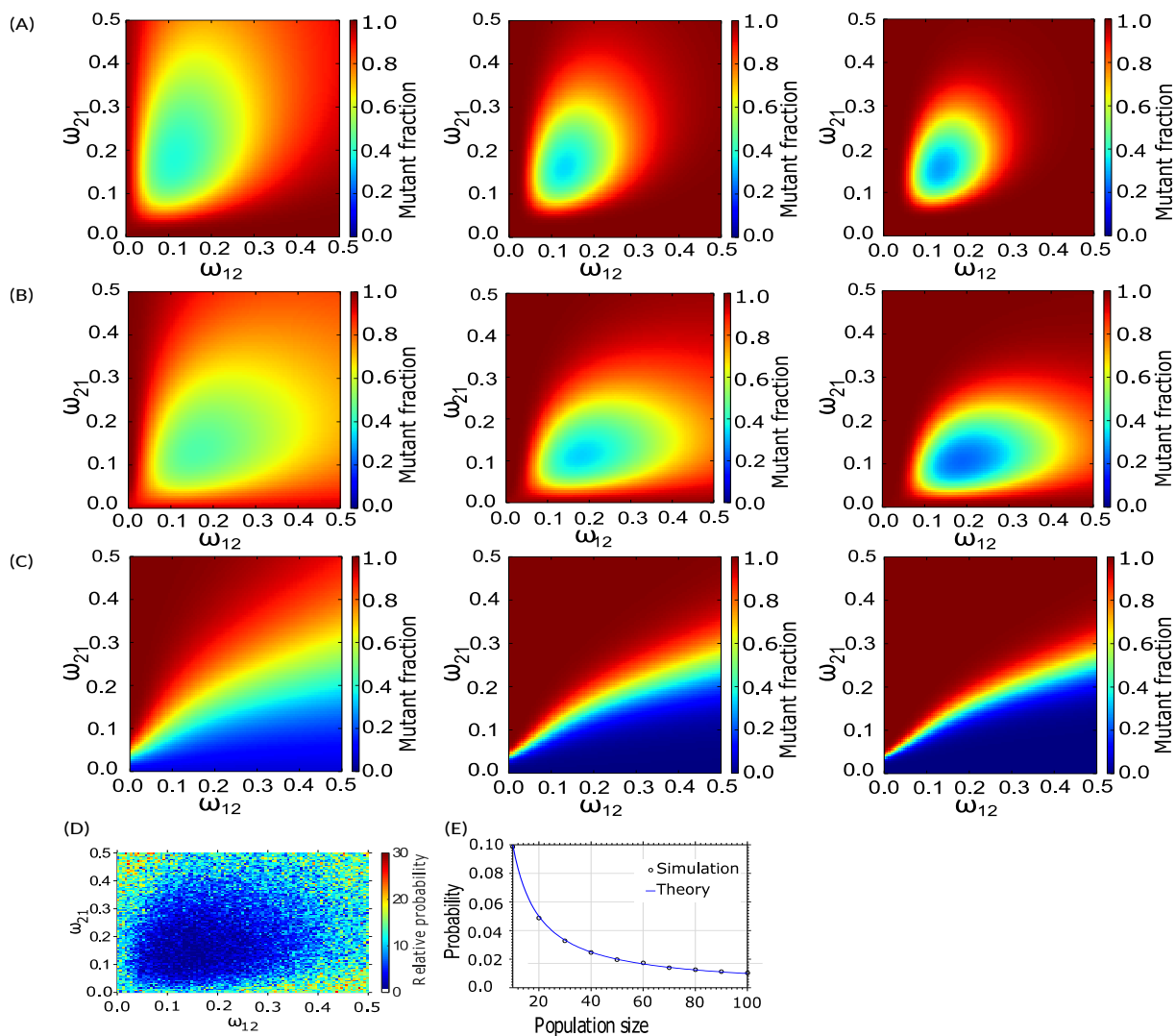

Figure 4. (Color), The fate of mutants that match their phenotypic switching rates with the rates of environmental fluctuations. We initiate a mutant whose switching rates are equal to the environmental switching rates, that is, ($\omega_{ij} = \frac{1}{\tau_j}$) in ancestral populations with various phenotypic switching rates. Points "N", "S" and "P" in Figure 3(A) are the conditions of the growth rates where mutant propagation was tested. (A B C) The snapshot of fraction of mutant population with growth rates located at point "P", "S" and "N" in Figure 3(A), respectively, at time period of $T = 25$, $T = 30$ & $T = 35$. As time progresses, the fraction of phenotype switching rate mutants expands to sweep almost all ancestral populations if the optimum occurs as assumed (A). (C, B) The same is not true if the assumed optimum is inadequate or invalid assumption. Here the mutants cannot always sweep the ancestral population. (D) The probability that a mutant invades the ancestral population relative to 1/N, the probability of invasion for neutral genetic drift, where N=100 is the population size. (E) Probability of invading the ancestral population for a neutral mutant as a function of the population size [25].

IV. Discussion

The idea that stochastic phenotypic switching can maximize the overall population fitness in temporally changing environments has been examined previously. Experimental and theoretical studies have proposed that the population fitness is maximal when the environmental switching rates match with the phenotypic switching rates [19]. However, all previous work assumed that the growth rate of each phenotype is much higher than the phenotypic switching rates. Here, we investigated the validity of the predicted optimal population growth rate using both deterministic and stochastic models of cellular growth. Our findings indicate that previously assumed optima are valid for low environmental switching rates (longer environmental durations and large growth rate difference in each environment). However, we also found broad parameter regimes where the assumed optimum was invalid. This was the case not only for shorter environmental durations (which was expected, since earlier models assumed slowly switching environments), but also when one of the environments suppressed the growth rates of both phenotypes. This is important, because stressful environments have exactly such an effect: they suppress growth of all cells in general, with some cells being suppressed less or perhaps being unaffected (but not enhanced). For example, antibiotic treatment strongly suppresses or kills fast-growing cells, while it suppresses minimally or does not affect the slow-growing persister cells. On the other hand, stress does not typically increase the division rates of slow-growing cells, which was the assumption for the original assumptions [19]. Finally, we also showed that a mutant which randomly hits the assumed fitness peak (matches its phenotypic switching rates with the environmental switching rates) can or cannot sweep the ancestral population depending on the validity of the fitness optimum assumption.

Further questions to explore include whether the optimal population growth rate is affected by cellular memory of the previous environment (meaning that cellular growth rates will take time to adjust to new values in new environments). Cellular growth rates in a given environment depend on various protein levels, which may take some time to adjust after an environmental shift. The effect of such delays may be more pronounced if the environmental durations are comparable to this type of cellular memory. Another open area is to make switching rates environment-dependent, as the growth rates are in the models discussed. This is justified, because cellular switching rates and growth rates may depend on the levels of the same protein, coupling both rates to the external environment [17].

V. Acknowledgments

VI. Appendix
A. Derivations

The population dynamics is governed by the equation

$$\frac{dX_i}{dt} = s_{ij}(\varepsilon)X_j, \tag{A1}$$

where $s_{ij}(\varepsilon)$ are elements of the matrix,

$$\mathbf{S}(\varepsilon) = \begin{bmatrix} g_1(\varepsilon) - \omega_{21} & \omega_{12} \\ \omega_{21} & g_2(\varepsilon) - \omega_{12} \end{bmatrix}.$$

The general solutions of such first order systems of ordinary differential equation are:

$$\mathbf{X}(\varepsilon,t) = c_1\mathbf{V}_1(\varepsilon)\exp(\lambda_1(\varepsilon)t) + c_2\mathbf{V}_2(\varepsilon)\exp(\lambda_2(\varepsilon)t), \tag{A2}$$

where $\lambda_i(\varepsilon)$ and $\mathbf{V}_i(\varepsilon)$ are eigenvalues and eigenvectors of $\mathbf{S}(\varepsilon)$, respectively.

Our goal is to determine c_1 and c_2 from initial conditions, when the population has N_1 and N_2 of type I and type II cells, respectively at $t = \tau_1$:

$$\begin{bmatrix} X_1(t = \tau_1) \\ X_2(t = \tau_1) \end{bmatrix} = \begin{bmatrix} N_1 \\ N_2 \end{bmatrix}.$$

The eigenvalues $\lambda_1(\varepsilon)$ and $\lambda_2(\varepsilon)$ are given by,

$$\lambda_{1,2}(\varepsilon) = \frac{\mathrm{Tr}(\mathbf{S}) \pm \sqrt{(\mathrm{Tr}(\mathbf{S}))^2 - 4\det(\mathbf{S})}}{2}, \tag{A3}$$

where $\mathrm{Tr}(\mathbf{S})$ and $\det(\mathbf{S})$ the trace and the determinant of $\mathbf{S}$, respectively.

Mathematically,

$\mathrm{Tr}(\mathbf{S}) = s_{11} + s_{22} = (g_1(\varepsilon) + g_2(\varepsilon)) - (\omega_{21} + \omega_{12})$ and

$\det(\mathbf{S}) = s_{11}s_{22} - s_{12}s_{21} = (g_1(\varepsilon) - \omega_{21})(g_2(\varepsilon) - \omega_{12}) - \omega_{21}\omega_{12} = g_1(\varepsilon)g_2(\varepsilon) - g_1(\varepsilon)\omega_{12} - g_2(\varepsilon)\omega_{21}$.

The corresponding eigenvectors are given by

$$\mathbf{V}_1(\varepsilon) = \begin{bmatrix} v_{11} \\ v_{21} \end{bmatrix} = \begin{bmatrix} \frac{1}{\sqrt{1 + \left(\frac{\lambda_1 - (g_1(\varepsilon) - \omega_{21})}{\omega_{12}}\right)^2}} \\ \frac{\frac{\lambda_1 - (g_1(\varepsilon) - \omega_{21})}{\omega_{12}}}{\sqrt{1 + \left(\frac{\lambda_1 - (g_1(\varepsilon) - \omega_{21})}{\omega_{12}}\right)^2}} \end{bmatrix}$$

and

$$\mathbf{V}_2(\varepsilon) = \begin{bmatrix} v_{12} \\ v_{22} \end{bmatrix} = \begin{bmatrix} \frac{1}{\sqrt{1 + \left(\frac{\lambda_2 - (g_1(\varepsilon) - \omega_{21})}{\omega_{12}}\right)^2}} \\ \frac{\frac{\lambda_2 - (g_1(\varepsilon) - \omega_{21})}{\omega_{12}}}{\sqrt{1 + \left(\frac{\lambda_2 - (g_1(\varepsilon) - \omega_{21})}{\omega_{12}}\right)^2}} \end{bmatrix}.$$

The time-dependent population state vectors can be written as

$$X_1(\varepsilon,t) = c_1 v_{11}(\varepsilon)\exp(\lambda_1(\varepsilon)t) + c_2 v_{12}(\varepsilon)\exp(\lambda_2(\varepsilon)t)$$
$$X_2(\varepsilon,t) = c_1 v_{21}(\varepsilon)\exp(\lambda_1(\varepsilon)t) + c_2 v_{22}(\varepsilon)\exp(\lambda_2(\varepsilon)t).$$

Solving at $t = \tau_1$ and setting $X_1(\tau) = N_1$, $X_2(\tau) = N_2$, yields,

$$\begin{bmatrix} N_1 \\ N_2 \end{bmatrix} = \mathbf{M} * \begin{bmatrix} c_1 \\ c_2 \end{bmatrix}, \tag{A4}$$

where

$$\mathbf{M} = \begin{bmatrix} v_{11}(\varepsilon)\exp(\lambda_1(\varepsilon)\tau_1) & v_{12}(\varepsilon)\exp(\lambda_2(\varepsilon)\tau_1) \\ v_{21}(\varepsilon)\exp(\lambda_1(\varepsilon)\tau_1) & v_{22}(\varepsilon)\exp(\lambda_2(\varepsilon)\tau_1) \end{bmatrix}.$$

Finally, since $\mathbf{M}$ is non-singular matrix, its inverse exists. Therefore,

we can invert equation (A4), results in the constants,

$$\begin{bmatrix} c_1 \\ c_2 \end{bmatrix} = \mathbf{M}^{-1} * \begin{bmatrix} N_1 \\ N_2 \end{bmatrix}. \tag{A5}$$

We solve the same system with different initial conditions determined by the number of cells in each subpopulation every time when the environment switches from ε_1 to ε_2 or vice versa.

B. Curve fitting

The plots in Figure 3(E) were fitted with a linear function, $p_1 g_2(\varepsilon_1) + p_2$, and exponential function, $ae^{bg_2(\varepsilon_1)}$, respectively. The parameters are then extracted and shown in table I.

parameter	$\tau_1 = \tau_2 = 5$	$\tau_1 = \tau_2 = 10$	$\tau_1 = \tau_2 = 15$	$\tau_1 = \tau_2 = 20$
p_1	-0.3039	-0.5100	-0.5208	-0.4333
p_2	0.3307	0.2857	0.2805	0.2551
a	3	53	1332	23480
b	-9.82	-14.98	-23.73	-28.54

Table I. Parameter values extracted from curve fitting.

[1] N. Balaban, J. Merrin, R. Chait, L. Kowalik, and S. Leibler, Science **305**, 1622 (2004).

[2] E. Kussell, R. Kishony, N. Balaban, and S. Leibler, Genetics **169**, 1807 (2005).

[3] A. Eldar and M. Elowitz, Nature **467**, 167 (2010).

[4] M. Kaern, T. Elston, W. Blake, and J. Collins, Nature Reviews Genetics **6**, 451 (2005).

[5] M. Elowitz, A. Levine, E. Siggia, and P. Swain, Science **297**, 1183 (2002).

[6] M. Acar, A. Becskei, and A. van Oudenaarden, Nature **435**, 228 (2005).

[7] N. Dhar and J. D. McKinney, Current Opinion in Microbiology **10**, 30 (2007).

[8] M. Harrison and D. Kreps, Journal of Economic Theory **20**, 381 (1979).

[9] A. Arkin, J. Ross, and H. McAdams, Genetics **149**, 1633 (1998).

[10] A. Oppenheim, O. Kobiler, J. Stavans, D. Court, and S. Adhya, Annual Review of Genetics **39**, 409 (2005).

[11] E. Ozbudak, M. Thattai, H. Lim, B. Shraiman, and A. van Oudenaarden, Nature **427**, 737 (2004).

[12] M. Kihara and R. Macnab, Journal of Bacteriology **145**, 1209 (1981).

[13] M. van der Woude and A. Bäumler, Clinical Microbiology Reviews **17**, 581 (2004).

[14] I. Henderson, P. Owen, and J. Nataro, Molecular Microbiology **33**, 919 (1999).

[15] D. Hilbert and P. Piggot, Microbiology and Molecular Biology Reviews **68**, 234 (2004).

[16] M. Yudkin and J. Clarkson, Molecular Microbiology **56**, 578 (2005).

[17] D. Nevozhay, R. Adams, E. Van Itallie, M. Bennett, and G. Balázsi, PLoS Computational Biology **8**, e1002480 (2012).

[18] M. Thattai and A. Van Oudenaarden, Genetics **167**, 523 (2004).

[19] E. Kussell and S. Leibler, Science **309**, 2075 (2005).

[20] B. Gaál, J. W. Pitchford, and A. J. Wood, Genetics **184**, 1113 (2010).

[21] D. Charlebois, J. Intosalmi, D. Fraser, and M. Kaern, Communications in Physics **9**, 89 (2011).

[22] S. Khalili, Y. Lin, A. Armaou, and T. Matsoukas, American Institute of Chemical Engineers **56**, 3137 (2010).

[23] N. Mantzaris, Journal of Theoretical Biology **241**, 690 (2006).

[24] N. Mantzaris, Biophysical Journal **92**, 4271 (2007).

[25] M. Kimura, Genetics **47**, 713 (1962).